Time development in quantum mechanics using a reduced Hilbert space approach

M. Belloni[a] and W. Christian[b]
Physics Department, Davidson College, Davidson, North Carolina 28035

(Received 3 September 2007; accepted 6 January 2008)

We have created a suite of open source programs that numerically calculate and visualize the evolution of arbitrary initial quantum-mechanical bound states. The calculations are based on the expansion of an arbitrary wave function in terms of basis vectors in a reduced Hilbert space. The approach is stable, fast, and accurate at depicting the long-time dependence of complicated bound states. Several real-time visualizations, such as the position and momentum expectation values and the Wigner quasiprobability distribution for the position and momentum, can be shown. We use these computational tools to study the time-dependent properties of quantum-mechanical systems and discuss the effectiveness of the algorithm. © *2008 American Association of Physics Teachers.*
[DOI: 10.1119/1.2837810]

I. INTRODUCTION

Wave packets, localized solutions of the Schrödinger equation, have been of interest since the beginning of quantum mechanics. It was Schrödinger[1] who first proposed a localized solution (a wave packet) to his wave equation as a way to study the connections between classical and quantum mechanics. Others soon found explicit wave packet solutions for localized quantum-mechanical "particles" subject to no force[2] (constant velocity) and a constant force[3] (constant acceleration), respectively. For a variety of reasons (such as the lack of computational power and lack of experimental verification), the study of wave packets lay dormant for many years. However, over the last 30 years quantum-mechanical wave packets and their revivals (the property that certain bound-state wave packets reform to their original shape in a predictable way) have received much theoretical attention and experimental verification.[4] In addition, quantum chaos[5] has emerged as a way to study quantum-mechanical systems whose classical counterparts exhibit chaos (even though the quantum-mechanical systems do not).

Many of these recent theoretical studies have focused on the long-time behavior of wave packets by utilizing specialized visualizations, such as the quantum carpet,[6] the Wigner distribution,[7] and, for quantum chaos, the Hussimi distribution.[8] These calculations and visualizations are often generated using a symbolic mathematical manipulation program to construct, evolve, and visualize energy eigenstates and their linear superpositions.

Although numerous computer programs and algorithms exist for the accurate numerical determination of energy eigenfunctions and eigenvalues,[9,10] the long-time evolution of arbitrary initial states is particularly difficult for position-space or momentum-space numerical algorithms to handle. To attain the necessary accuracy the spatial grid and the time steps used must be very small, and hence it takes many computations to reach the revival time scale. As a result, numerical errors accumulate and, although the algorithms are stable because they conserve probability, they cease to be accurate enough to show important long-time features of the quantum-mechanical state.

To address these issues we have developed a suite of open-source simulations as part of the Open Source Physics Project.[11] These programs simulate the time evolution based on the expansion of an arbitrary wave function in terms of the basis vectors in a reduced Hilbert space.[12] Because the programs are based on the superposition principle, many of the drawbacks we have described of standard numerical algorithms do not arise, allowing for the visualization of wave packets. The programs make the creation and study of quantum-mechanical superpositions easy and accessible for students and instructors.

II. REVIEW OF TIME-EVOLUTION ALGORITHMS

The time-dependent quantum mechanical wave function is inherently complex (here in one dimension and in position space):

$$\left[-\frac{\hbar^2}{2m}\frac{\partial^2}{\partial x^2}+V(x)\right]\Psi(x,t)=i\hbar\frac{\partial}{\partial t}\Psi(x,t). \tag{1}$$

The evolution of an arbitrary state is given by

$$\Psi(x,t)=e^{-i\hat{\mathcal{H}}(t-t_0)/\hbar}\Psi(x,t_0), \tag{2}$$

where the operator $\hat{\mathcal{H}}=-\frac{\hbar^2}{2m}\frac{\partial^2}{\partial x^2}+V(x)$ is the Hamiltonian.

To solve Eq. (1) for an arbitrary potential energy function, we first specify the wave function $\Psi(x,t_0)$ at some initial time t_0 and then evolve it in time as

$$\Psi(x,t_0+\Delta t)=e^{-i\hat{\mathcal{H}}(\Delta t)/\hbar}\Psi(x,t_0), \tag{3}$$

where Δt is the time step.

Standard approaches such as Crank–Nicolson,[13] Numerov,[14] split operator, and staggered-time (also called half-step),[15] accomplish this update in a variety of ways.[16] These algorithms are successful since they are inherently stable since they conserve probability and energy. However, for long times numerical errors begin to accumulate and the results will eventually deviate from the "true" results. The accumulation of errors is most often found in the inaccurate depiction of the shape of the wave function and the phase. Such inaccuracies can mask the often subtle long-time features of quantum-mechanical systems and limit these algorithms to the study of short times.

III. THE REDUCED HILBERT SPACE APPROACH

In the reduced Hilbert space approach,[17] more generally called the spectral method,[18] the basis set of Hilbert space,

which is typically an infinite dimensional space, is limited to some finite dimension N. As a practical matter we rarely construct a complete Hilbert space, and such a construction is often impractical or impossible. Because of finite computer resources, we cannot create an infinite number of basis vectors to represent a complete Hilbert space, but for many problems it suffices to have a reduced Hilbert space. To see how this reduction will (or won't) affect the end result, we construct two projection operators,

$$\hat{\mathcal{P}}_N = \sum_{n=1}^{N} |\psi_n\rangle\langle\psi_n| \tag{4}$$

and

$$\hat{\mathcal{P}}_D = \sum_{n=N+1}^{\infty} |\psi_n\rangle\langle\psi_n|, \tag{5}$$

where the sum of the two projection operators in Eqs. (4) and (5) is the complete projection operator, $\hat{\mathcal{P}}$. We consider an arbitrary initial state $|\Psi\rangle$ and define

$$|\Psi_N\rangle \equiv \hat{\mathcal{P}}_N|\Psi\rangle \text{ and } |\Psi_D\rangle \equiv \hat{\mathcal{P}}_D|\Psi\rangle, \tag{6}$$

which describes the part of the original wave function that is in the reduced Hilbert space and the part that is not. We can write

$$\hat{\mathcal{H}}|\Psi\rangle = \hat{\mathcal{H}}(\hat{\mathcal{P}}_N + \hat{\mathcal{P}}_D)(\hat{\mathcal{P}}_N + \hat{\mathcal{P}}_D)|\Psi\rangle \tag{7a}$$

$$= \hat{\mathcal{H}}\hat{\mathcal{P}}_N|\Psi_N\rangle + \hat{\mathcal{H}}\hat{\mathcal{P}}_D|\Psi_D\rangle, \tag{7b}$$

because $\hat{\mathcal{P}}_N + \hat{\mathcal{P}}_D = \hat{\mathcal{P}} = \hat{\mathcal{I}}$ and $\hat{\mathcal{P}}_N|\Psi_D\rangle = \hat{\mathcal{P}}_D|\Psi_N\rangle = 0$.

We now construct the complete Schrödinger equation for $|\Psi_D\rangle$ and $|\Psi_N\rangle$ by operating $\hat{\mathcal{P}}_N$ and $\hat{\mathcal{P}}_D$ on Eq. (1) using Eq. (7b):

$$\hat{\mathcal{P}}_N\hat{\mathcal{H}}\hat{\mathcal{P}}_N|\Psi_N\rangle + \hat{\mathcal{P}}_N\hat{\mathcal{H}}\hat{\mathcal{P}}_D|\Psi_D\rangle = i\hbar\frac{\partial}{\partial t}|\Psi_N\rangle \tag{8}$$

and

$$\hat{\mathcal{P}}_D\hat{\mathcal{H}}\hat{\mathcal{P}}_N|\Psi_N\rangle + \hat{\mathcal{P}}_D\hat{\mathcal{H}}\hat{\mathcal{P}}_D|\Psi_D\rangle = i\hbar\frac{\partial}{\partial t}|\Psi_D\rangle. \tag{9}$$

If in our computations (by virtue of the state, $|\Psi\rangle$ selected), $|\Psi_D\rangle$ is vanishingly small, then we are left with

$$\hat{\mathcal{P}}_N\hat{\mathcal{H}}\hat{\mathcal{P}}_N|\Psi_N\rangle = i\hbar\frac{\partial}{\partial t}|\Psi_N\rangle, \tag{10}$$

which when integrated yields

$$|\Psi_N(t)\rangle = e^{-i\hat{\mathcal{P}}_N\hat{\mathcal{H}}\hat{\mathcal{P}}_N t/\hbar}|\Psi_N(0)\rangle. \tag{11}$$

If we can compute a precise subset of energy eigenvectors $\{\psi_n\}$, $[\mathcal{H},\mathcal{P}_N]=0$, because the projection operator is constructed from these energy eigenvectors. Equation (11) then simplifies to

$$|\Psi_N(t)\rangle = e^{-i\hat{\mathcal{H}}t/\hbar}|\Psi_N(0)\rangle = e^{-i\hat{\mathcal{H}}t/\hbar}\hat{\mathcal{P}}_N|\Psi(0)\rangle \tag{12a}$$

$$= \sum_{n=1}^{N} e^{-iE_n t/\hbar}|\psi_n(0)\rangle\langle\psi_n(0)|\Psi(0)\rangle, \tag{12b}$$

where $c_n \equiv \langle\psi_n(0)|\Psi(0)\rangle$. Hence, $|\Psi_N(t)\rangle = \Sigma_{n=1}^{N} c_n e^{-iE_n t/\hbar}|\psi_n(0)\rangle$.

The construction of a linear superposition in position space using the reduced Hilbert space approach proceeds like the usual case for a linear superposition of energy eigenstates as long as we satisfy two conditions: (1) the Hilbert space is large enough so that a finite subset of basis states is sufficient to properly represent the initial state and (2) we have accurate energy eigenfunctions $\psi_n(x)$ and energy eigenvalues E_n corresponding to the potential energy function $V(x)$. Energy eigenfunctions and eigenvalues can be computed using a numerical algorithm if analytic expressions are unavailable.

IV. PROGRAM DESCRIPTION

The QMSUPERPOSITION program solves Eq. (1) by first creating a table of energy eigenfunctions and eigenvalues of the time-independent Schrödinger equation in position space (using units where $\hbar=2m=1$), and then creating linear superpositions of such states. Because the infinite square well, simple harmonic oscillator, and infinite well with periodic boundary conditions are standard problems with well-known analytic solutions, the energy eigenfunctions and eigenvalues associated with these potential energy functions are coded into the program. If an arbitrary potential energy function is chosen, the program determines the energy eigenfunctions and eigenvalues via the shooting method with hard (infinite) walls at the positions xmin and xmax.

As shown in Fig. 1 and in more detail in Table I, the QMSUPERPOSITION program allows the user to change several input parameters. For example, in the $V(x)$ dialog box well, sho, or ring can be chosen, and the program will use the analytic energy eigenfunctions and eigenvalues for the infinite square well, the harmonic oscillator, or the infinite well with periodic boundary conditions, respectively. For any user-defined potential energy function, the program will calculate the energy eigenfunctions and eigenvalues numerically. For example, an asymmetric infinite square well can be simulated by setting xmin=−3, xmax=3, and $V(x)$ =100∗step(x), where step(x) denotes the Heaviside step function, $\theta(x)$.

A superposition is then constructed based on the real and imaginary components of the expansion coefficients, c_n, which the user supplies in a comma-delimited list,

$$\mathrm{Re}\{c_n\} = \{a_1, a_2, a_3, a_4, \ldots, a_N\} \tag{13a}$$

and

$$\mathrm{Im}\{c_n\} = \{b_1, b_2, b_3, b_4, \ldots, b_N\}. \tag{13b}$$

The wave function and its time evolution is then determined by the weighted sum of the individual energy eigenfunctions according to $\Psi(x,t)=\Sigma_{n=1}^{N} c_n e^{-iE_n t/\hbar}\psi_n(x)$. The user determines the appropriate value of N by the size of the comma-delimited list. Therefore a single eigenstate, a two-state superposition, or a wave packet can be displayed by changing c_n. The resulting wave function can be visualized either by viewing the real and imaginary parts separately or by viewing in amplitude and phase, where the phase is depicted as color superimposed on the amplitude.

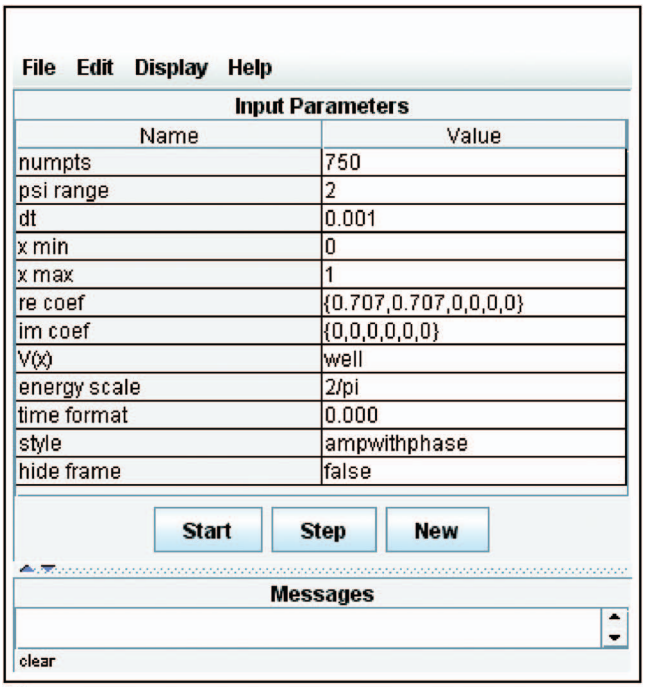

(a)

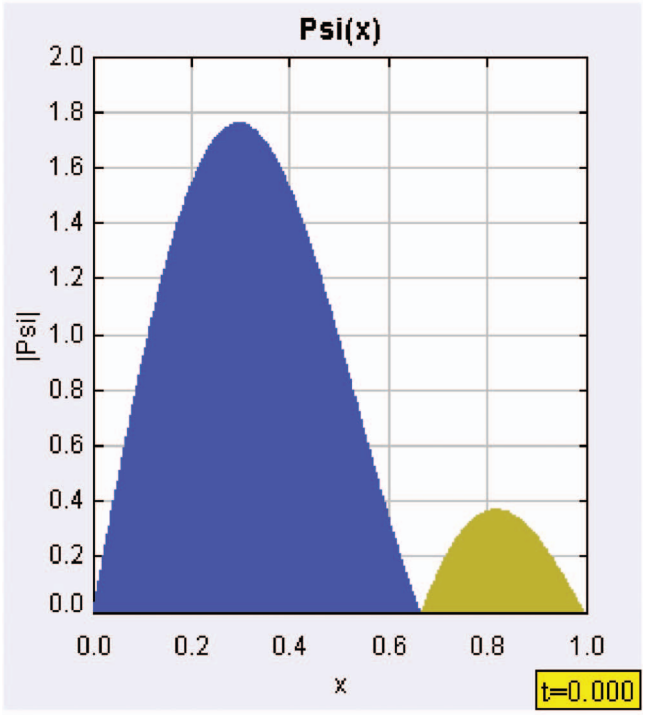

(b)

Fig. 1. The QMSuperposition program showing an equal superposition of $n=1$ and $n=2$ states in the infinite square well. (a) The user interface. (b) The wave function in the color-as-phase representation. We choose units such that $\hbar=2m=1$ for all the figures.

The QMPROJECTION program (see Fig. 2) can be used to compute the expansion coefficients for an arbitrary initial wave function. The user enters $\Psi(x,0)$, the wave function at $t=0$, the potential energy function, and the appropriate value of N. This program, like QMSUPERPOSITION, first determines the energy eigenfunctions and eigenvalues (whether analytic or numeric), and then numerically calculates the expansion coefficients via

$$c_n = \int_{x_{\min}}^{x_{\max}} \psi_n^*(x)\Psi(x,0)dx. \tag{14}$$

Once the coefficients are determined, the time evolution of the wave function proceeds like that of QMSUPERPOSITION. These calculations are all done initially and then stored, so the time delay associated with computing the reduced Hilbert space and the expansion coefficients occurs only once, when the program is loaded.

As described in Ref. 19, open source physics programs can save and read XML parameter files. Therefore, we can create, store, and reload complicated superpositions. Because curriculum authors and instructors may wish to hide input parameters, the programs listed in Table II are available with a simplified user interface that does not display the parameter input table. To distinguish between these versions, the program name ends in App (our convention for **app**lications) or WRApp (a "**wr**apped up" **app**lication). Programs with the simple interface can read XML data files created with the standard interface. For comparison, Figs. 1 and 2 show the standard application (App) interface and Figs. 3–5 show the interface with just the Start/Stop, Step, Reset buttons (WRApp).

Open Source Physics programs can be accessed by obtaining the source code or running applets from the Web. An easier way to use these programs is to download compiled versions packaged within an executable Java archive called a jar file. The materials described in this paper are contained in ajp_reduced_hilbert.jar. Clicking on the jar file executes a program called LAUNCHER. LAUNCHER is a Java application that can run other Java programs. We use LAUNCHER to organize and distribute collections of ready-to-use programs, documentation, and curricular material in a single easily modifiable package. Delivering curricular material in LAUNCHER packages has the advantage of being self-contained and only dependent on having Java installed on a local machine and not on the type of operating system or browser.

Table I. Input parameters for the QMSuperposition program.

Parameter	Description
numpts	number of points used to plot the wave function
psi range	y, range of the visualization
dt	time step
xmin	left edge of the well
xmax	right edge of the well
re coef	real part of the expansion coefficients
im coef	imaginary part of the expansion coefficients
$V(x)$	potential energy function
energy scale	scale of the energy and hence the time evolution
time format	format for the time display
shooting tolerance	tolerance for the shooting method calculation
style	display style for the wave function

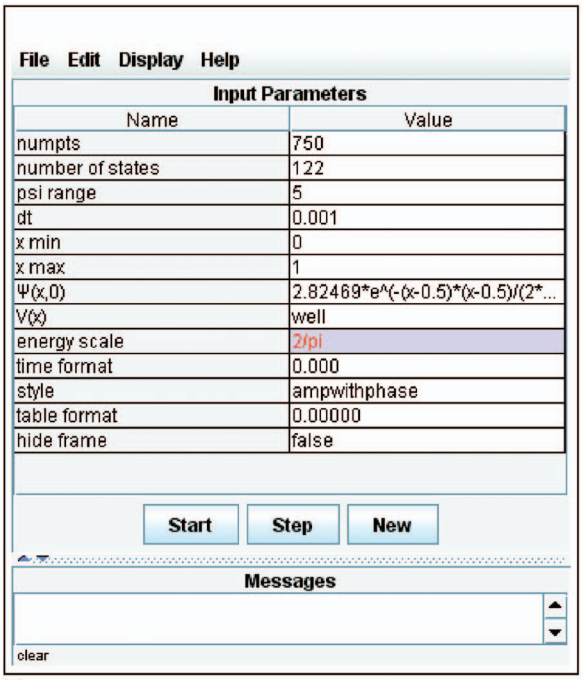

(a)

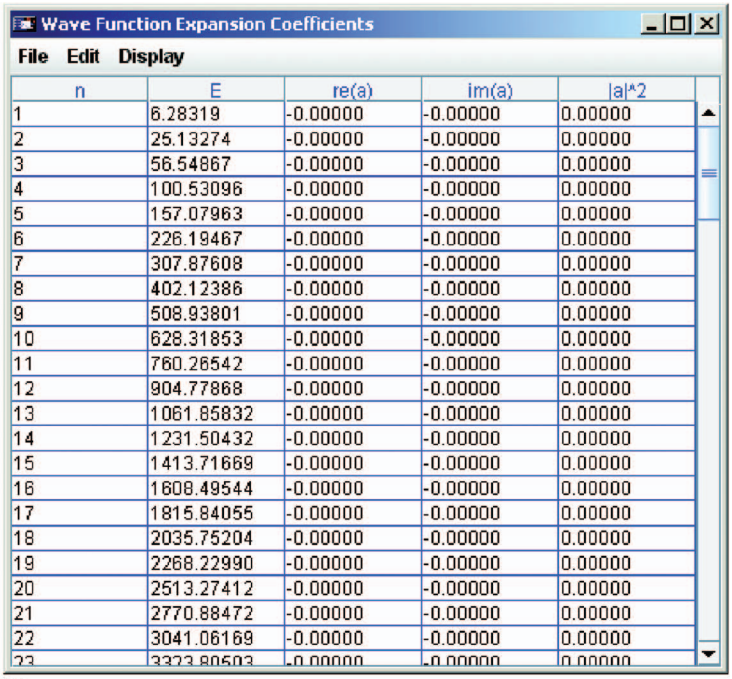

(b)

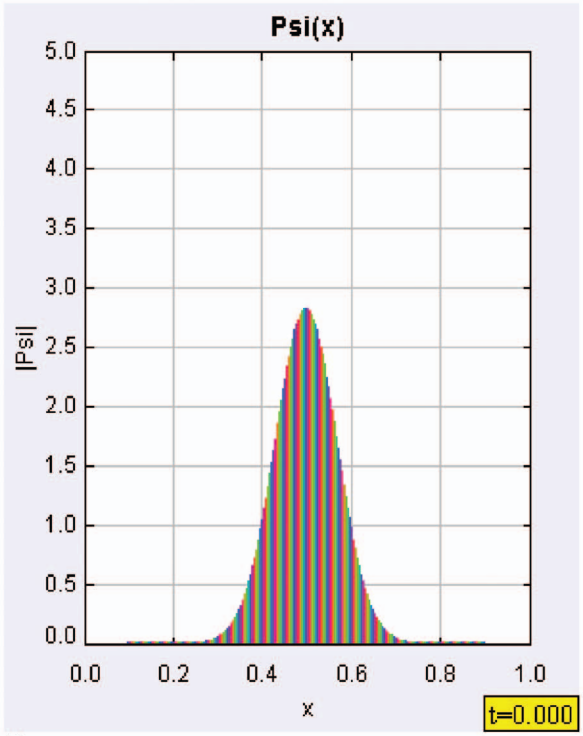

(c)

Fig. 2. (a) The QMProjection user interface showing the parameters for an initial Gaussian wave packet in the infinite square well. (b) Table of the energies and the real and imaginary parts of the expansion coefficients calculated by the program. The square of the expansion coefficient amplitudes $|c_n|^2$ is also shown. Due to the high initial momentum of the packet $N=122$, the first 60 expansion coefficients are zero as shown. (c) The resulting wave function.

V. VISUALIZATIONS

Thus far we have focused on the ability of QMSUPERPOSITION to construct and display quantum-mechanical wave functions. In addition to this main program, there are numerous subclasses of the main program that add additional problem-specific visualizations.

PROBABILITYAPP shows the probability density, and FFTAPP shows the momentum-space wave function using the fast Fourier transform:[20]

$$\phi(p,t) = \frac{1}{\sqrt{2\pi\hbar}} \int_{-\infty}^{+\infty} \psi(x,t) e^{-ipx/\hbar} dx. \tag{15}$$

Table II. Open Source Physics programs that use the reduced Hilbert space approach.

Program	Description
QMSuperposition	wave function
ProbabilityApp	probability density
ExpectationXApp	$\langle x \rangle$
ExpectationPApp	$\langle p \rangle$
FFTApp	momentum-space wave function
CarpetApp	position-space quantum carpet
MomentumCarpetApp	momentum-space quantum carpet
WignerApp	Wigner function
ProjectionApp	calculation of expansion coefficients
MeasurementApp	quantum-mechanical measurement

As shown in Fig. 3, the EXPECTATIONXAPP and EXPECTATIONPAPP programs display the time development of $\langle \hat{x} \rangle$ and $\langle \hat{p} \rangle$ alongside the wave function. These visualizations show the relation via Ehrenfest's principle, $\langle \hat{p} \rangle_t = m d\langle \hat{x} \rangle_t / dt$, of quantum-mechanical expectation values and classical trajectories. The CARPETAPP and MOMENTUMCARPETAPP programs display quantum carpets (spacetime diagrams of the wave function).

More specialized visualizations, such as the Wigner quasiprobability distribution function[7] for quantum phase space,

$$P_W(x,p;t) \equiv \frac{1}{\pi\hbar}\int_{-\infty}^{+\infty} \psi^*(x+y,t)\psi(x-y,t)e^{2ipy/\hbar}dy, \quad (16)$$

are available. Figure 4 shows the energy eigenfunction and the resulting Wigner distribution for the $n=10$ energy eigenstate of an infinite square well. Note that although the Wigner function $P_W(x,p;t)$ is real, it almost always has small regions of phase space ($\Delta x \Delta p \approx \hbar$) where it is negative. Only single Gaussian wave packets are known[22] to give rise to nonnegative Wigner functions. The negative values when wave functions evolve away from a Gaussian shape is a feature of the noncommutativity of $\hat{x}$ and $\hat{p}$ encoded in the uncertainty principle.[23]

VI. EXAMPLES

To show results from the programs and to touch base with the research literature, we show in Figs. 2, 3, 5, and 6 the time evolution of an initially localized state using a standard Gaussian wave packet,

$$\Psi(x,0) = \frac{1}{\sqrt{\alpha\sqrt{\pi}}} e^{-(x-x_0)^2/2\alpha^2} e^{ip_0(x-x_0)/\hbar}, \quad (17)$$

in an infinite square well. We choose units and well parameters such that $2m=L=\hbar=1$ and set $x_0=0.5L=0.5$, $p_0=80\pi\hbar/L=80\pi$, and $\alpha=1/10\sqrt{2}=0.0707$. Given that $\Delta x_0=\alpha/\sqrt{2}=1/20$, the initial width of the packet is small enough to contain the packet within the infinite square well (the Gaussian packet is vanishingly small at and beyond the walls). We project this wave function into Hilbert space and find that a reduced Hilbert space with $N=120$ is sufficient so that all remaining coefficients are of order 10^{-10} or smaller.

A characteristic time scale of a quantum-mechanical wave packet in an infinite square well is the classical period $T_{\rm cl}$,

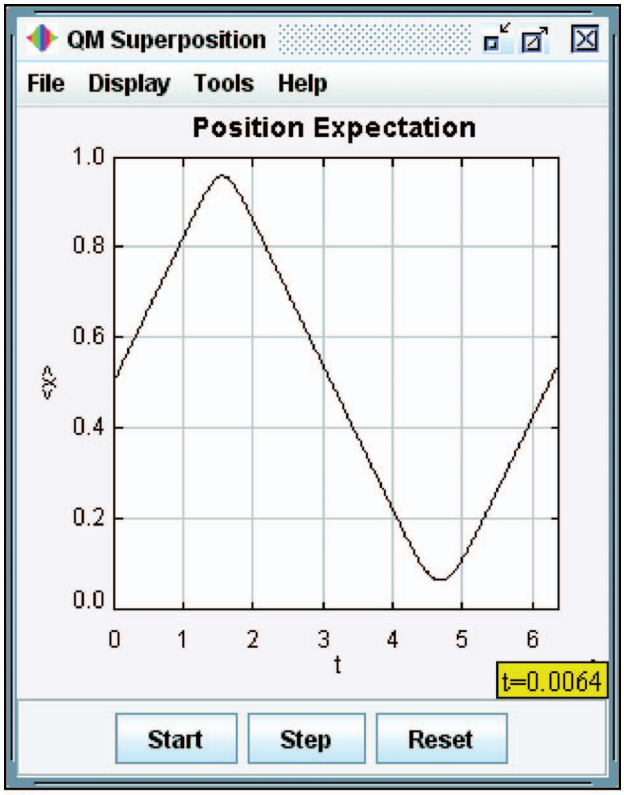

(a)

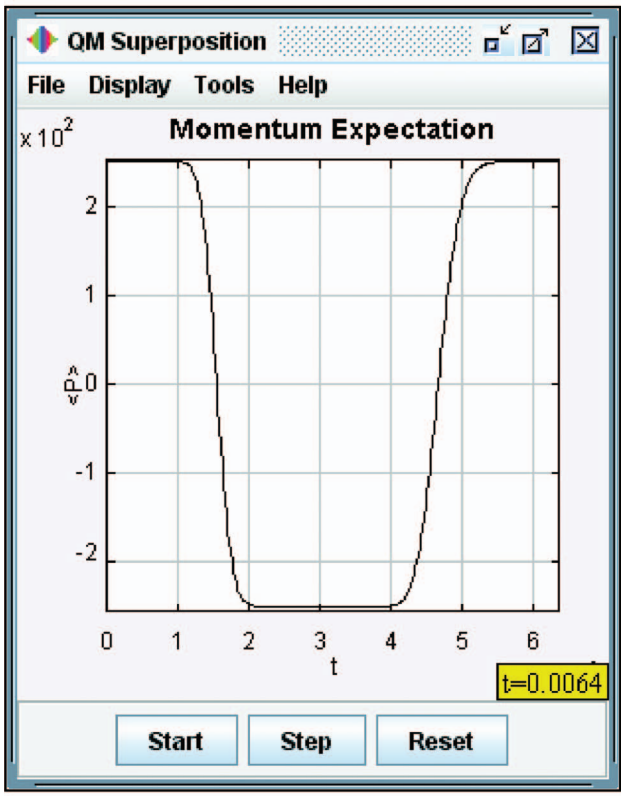

(b)

Fig. 3. The QMSuperpositionExpectationX and QMSuperpositionExpectationP programs display the expectation values (a) $\langle \hat{x} \rangle$ and (b) $\langle \hat{p} \rangle$ versus t. Note the simplified controls of the WRApp version of the programs. Here the programs are used to depict the short-time evolution of a Gaussian wave packet in an infinite square well (Ref. 21) showing that, for this time frame, the quantum-mechanical expectation values still closely mimic $x(t)$ and $p(t)$ for a classical particle in an infinite well.

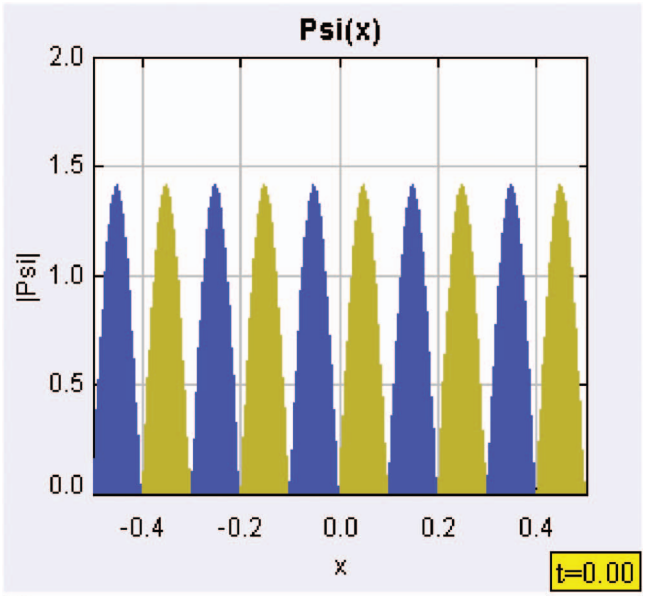

(a)

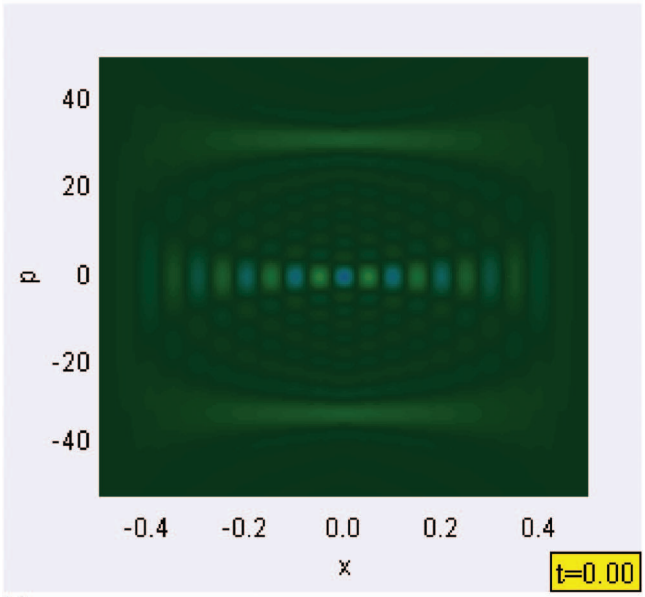

(b)

Fig. 4. The QMSuperpositionWigner program showing the (a) energy eigenfunction and (b) the resulting Wigner distribution for the $n=10$ energy eigenstate in an infinite square well. The Wigner function image matches Fig. 4 in Ref. 24.

$$T_{\mathrm{cl}} = \frac{2L}{p_0/m} = \frac{1}{80\pi}. \tag{18}$$

The short-term behavior of the expectation values $\langle \hat{x} \rangle$ and $\langle \hat{p} \rangle$ of the Gaussian wave packet shown in Fig. 3 has this period.

The long-time dependence of any quantum state is determined by the complex exponentials, $\exp(-iE_n t/\hbar)$, which are directly related to the energies of the individual states.[25] For the infinite square well, these energies are $E_n = n^2\pi^2\hbar^2/2mL^2$ or $E_n = n^2\pi^2$ in units where $\hbar = 2m = 1$. Because all energy eigenvalues are integer multiples of the ground state energy, the complex exponentials produce phase oscillations that are harmonics of the ground state phase oscillation resulting in revivals.

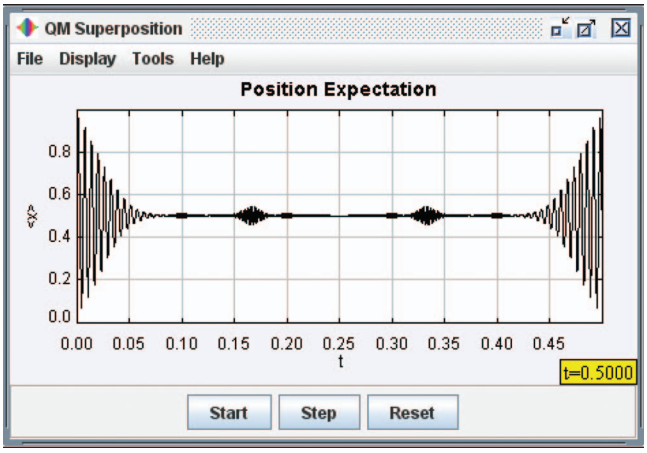

Fig. 5. The QMSuperpositionExpectationX program showing $\langle \hat{x} \rangle$ versus t for the long-time evolution of a Gaussian wave packet in an infinite square well. The results match Fig. 7 in Ref. 28. The corresponding wave functions at $t = T_{\mathrm{rev}}/3$ and $t = T_{\mathrm{rev}}/2$ are shown in Fig. 6.

The time it takes each of the $\exp(-iE_n t/\hbar)$ factors to undergo one complete revolution in the complex plane [for $\exp(-iE_n t/\hbar) = 1$] is $T_n = 2\pi/E_n$; the longest such time is identified as the revival time $T_{\mathrm{rev}} = T_1$. For the well we are considering, we find $T_n = 2/\pi n^2$. Because the E_n and the T_n are integers or integer fractions of E_1 and T_{rev}, respectively, the $\exp(-iE_n t/\hbar)$ factors are all unity at the revival time $T_{\mathrm{rev}} = 2/\pi$, and hence the wave packet returns to its exact initial state. At $t = T_{\mathrm{rev}}/2$, the wave packet reforms with the same shape but at a "mirrored" location and with a mirrored momentum. At other times, pT_{rev}/q, where p and q are integers, the wave packet can also reform as several "mini-packets" of the original wave packet.[26] The long-time revival behavior of this wave packet is shown via the expectation value of x in Figs. 5 and 6.[27,28] In all our examples, we have scaled the time to make the revival time, T_{rev}, equal to 1.

VII. ACCURACY OF THE ALGORITHM

It is instructive to examine the effect of errors on the computation of the reduced Hilbert space by the shooting method.[29] That is, how good does the shooting method have to be to accurately depict the initial wave function and depict the long-time behavior of the wave function ($t > T_{\mathrm{rev}}$) and how do the energy eigenfunction and eigenvalue errors manifest themselves?

The shooting tolerance input parameter in our programs controls both the tolerance of the Runge–Kutta–Fehlberg 4/5 ordinary differential equation solver,[30] which computes the shape of the energy eigenfunctions, and the bisection algorithm,[31] which computes the energy eigenvalues. Once the packet is constructed from these energy eigenfunctions and eigenvalues, the QMPROJECTION program gives a measure of the point-by-point degradation of the shape of the constructed wave function, $\tilde{\Psi}(x,0)$, compared to the input wave function, $\Psi(x,0)$, via

$$\text{projection error} = \sqrt{\sum_{\text{points}} |\tilde{\Psi}(x,0) - \Psi(x,0)|^2 \, \Delta x}. \tag{19}$$

For a suitable number of points greater than 100 and at least five times the maximum quantum number in the superposi-

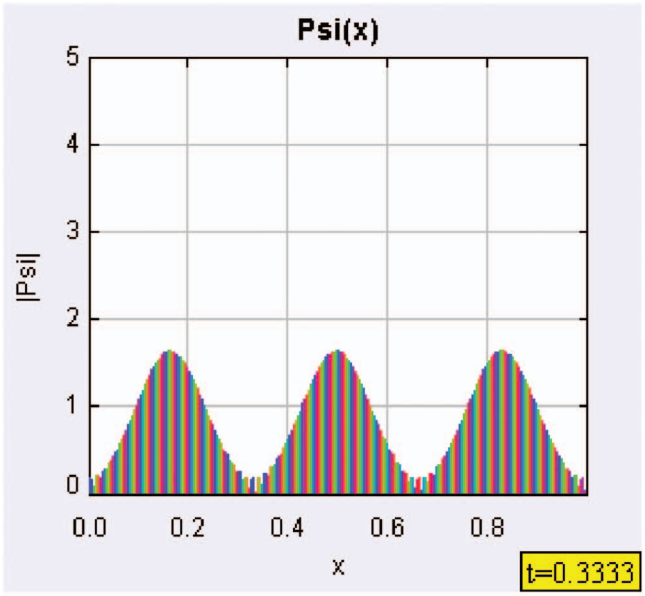

Fig. 6. The QMSuperpositionApp program depicting the fractional revivals at (a) $t=T_{\text{rev}}/3$ and (b) $t=T_{\text{rev}}/2$ of a Gaussian wave packet in an infinite square well using a reduced Hilbert space, $N=120$, computed with 1000 points and a shooting tolerance of 10^{-6}.

tion N, the calculated projection error is on the order of the shooting tolerance. A projection error of less than 0.005 yields no noticeable difference between the shape of the constructed and input wave functions.

A discretized x-coordinate space limits the wave function resolution as well as enforces infinite square well boundary conditions at the end points. Accurate bound-state energy eigenfunctions and eigenvalues can still be computed if the potential well is sufficiently deep so that the energy eigenfunction decays to the shooting tolerance before it reaches the end points. For example, the shooting method solution for $\hbar=2m=1$ and $V(x)=4x^2$ with $x_{\min}=-\pi/\sqrt{2}$ and $x_{\max}=\pi/\sqrt{2}$ gives energy eigenvalues $E_1=2.000\,691\,161$, $E_2=6.011\,955\,872$, and $E_3=10.090\,518\,6$ in excellent agreement with the exact solution of the two-mode harmonic oscillator-infinite square well system of Ref. 32. The simulation also confirms the harmonic oscillator and infinite square well limits of this two-mode system for small and large quantum numbers, respectively.

We can understand the eventual numerical breakdown of the revival behavior by considering the numerical values of the individual energies as they appear in the exponentials, $\exp(-iE_nt/\hbar)$. In this case, the precise shape of the eigenfunctions is not as important as the values of the energy eigenvalues because a deviation ΔE_n from the correct energy will cause a phase drift of each term in the expansion. The time during which all of the states in the superposition maintain their correct relative phases is analogous to the coherence time in optics. The effect of the phase drift is largest for the term with the largest value of $|c_n|^2$ in the expansion. For the Gaussian wave packet example used in Fig. 6, the term with the largest value of $|c_n|^2$ corresponds to $n_0=80$. For this packet a deviation in the energy, $|\Delta E_{n_0}|\geq 0.01$, will create a noticeable deviation at the revival time. In our numerical tests with the Gaussian wave packet using 1000 points, a shooting tolerance of 10^{-6} results in the numerically computed wave packet losing its Gaussian shape after three revival periods.

For comparison, at $t=0$ the projection error and the energy deviation are both 5×10^{-11} for the analytically determined packet. Although these errors are vanishingly small, they are nonzero due to the finite precision arithmetic inherent in any computer calculation. Therefore, selecting analytic solutions to construct the reduced Hilbert space gives an (almost) perfect initial wave function and a very long coherence time.

VIII. CONCLUSIONS AND DISCUSSIONS

We have briefly described the suite of open source programs that use the reduced Hilbert space approach for depicting the long-time behavior of quantum-mechanical systems. The approach is fast and reliable. We have focused on the long-time evolution of initially localized states in the infinite square well as a way to illustrate results from the literature. Other programs on the OPEN SOURCE PHYSICS website simulate quantum measurement[19] and the time evolution of two-dimensional wave functions in (separable) potentials. Because our programs are open source and modular, it is easy to add new visualizations. The programs can be used as a quick and effective way to test parameters for the study of wave packets in quantum wells for which analytic solutions of the energy eigenfunctions and eigenvalues are unavailable.

The compiled programs described in this paper are available on EPAPS[33] as a Launcher package. Additional packages with supporting curricular materials based on these and related programs (including other wells and quantum-mechanical measurement and spin) are available online on the quantum exchange in ComPADRE,[34] the quantum mechanics section of that digital library (search for OPEN SOURCE PHYSICS or OSP) and the OPEN SOURCE PHYSICS and BQLearning websites.[11] On these sites the simulations and curricular materials can be accessed as individual exercises, as smaller parts organized by topic, or as the entire package and supporting worksheets. Both the ComPADRE and BQLearning sites are categorized by topic and allow for

searching by topic, by author (search for OPEN SOURCE PHYSICS or OSP), and by numerous other fields.

ACKNOWLEDGMENT

The Open Source Physics Project is supported by the National Science Foundation (Grant No. DUE-0442581).

[a]Electronic mail: mabelloni@davidson.edu
[b]Electronic mail: wochristian@davidson.edu

[1] E. Schrödinger, "Der stetige Übergang von der Mikro- zur Makromechanik," Naturwissenschaften **14**, 664–666 (1926); translated and reprinted as "The continuous transition from micro- to macro mechanics," in *Collected Papers on Wave Mechanics* (Chelsea Publishing, NewYork, 1982), pp. 41–44.
[2] C. G. Darwin, "Free motion in the wave mechanics," Proc. Roy. Soc. A **117**, 258–293 (1928).
[3] E. H. Kennard, "The quantum mechanics of an electron or other particle," J. Franklin Inst. **207**, 47–78 (1929); See also "Zur Quantenmechanik einfacher Bewegungstypen" ("The quantum mechanics of simple types of motion"), Z. Phys. **44**, 326–352 (1927).
[4] For an extensive review of the historical, experimental, and theoretical background of wave packet dynamics see R. W. Robinett, "Quantum wave packet revivals," Phys. Rep. **392**, 1–119 (2004).
[5] H. J. Stöckmann, *Quantum Chaos: An Introduction* (Cambridge U.P., Cambridge, 1999).
[6] I. Marzoli, F. Saif, I. Bialynicki-Birula, O. M. Friesch, A. E. Kaplan, and W. P. Schleich, "Quantum carpets made simple," Acta Phys. Slov. **48**, 323–333 (1998), or arXiv:quant-ph/9806033.
[7] E. Wigner, "On the quantum correction for thermodynamic equilibrium," Phys. Rev. **40**, 749–759 (1932).
[8] K. Takahashi and N. Saitô, "Chaos and Husimi distribution function in quantum mechanics," Phys. Rev. Lett. **55**, 645–648 (1985).
[9] William H. Press, Saul A. Teukolsky, William T. Vetterling, and Brian P. Flannery, *Numerical Recipes in* C++*: The Art of Scientific Computing* (Cambridge U. P., Cambridge, 2002), 2nd ed.
[10] Harvey Gould, Jan Tobochnik, and Wolfang Christian, *Introduction to Computer Simulation Methods* (Addison–Wesley, San Francisco, 2006), pp. 673–721.
[11] ⟨www.opensourcephysics.org/apps/qm/⟩ and ⟨www.bqlearning.org/⟩.
[12] The only other simulations that are based on the superposition principle that we could find are available at ⟨www.atm.ox.ac.uk/user/palmer/Applet.html⟩ and ⟨www.falstad.com/qm1d/⟩.
[13] J. R. Hiller, I. D. Johnston, and D. F. Styer, *Quantum Mechanics Simulations: The Consortium for Upper-Level Physics Software* (Wiley, New York, 1995).
[14] J. L. Friar, "A note on the roundoff error in the Numerov algorithm, "J. Comput. Phys. **28**, 426–432 (1978).
[15] P. B. Visscher, "A fast explicit algorithm for the time-dependent Schrödinger equation," Comput. Phys. **5**, 596–598 (1991).
[16] C. Leforestier *et al.*, "A comparison of different propagation schemes for the time dependent Schrödinger equation," J. Comput. Phys. **94**, 59–80 (1991).
[17] D. J. Tannor, *Introduction to Quantum Mechanics: A Time-Dependent Perspective* (University Science Books, Sausalito, 2007), Chap. 11.
[18] D. Gottlieb and S. A. Orszag, *Numerical Analysis of Spectral Methods: Theory and Applications* (Society for Industrial Mathematics, Philadelphia, 1987).
[19] W. Christian, M. Belloni, and D. Brown, "An open source XML framework for authoring curricular material," Comput. Sci. Eng. **8**, 51–58 (2006); M. Belloni, W. Christian, and D. Brown, "Open Source Physics curricular material for quantum mechanics: Dynamics and measurement of quantum two-state superpositions," Comput. Sci. Eng. **9**, 24–31 (2007).
[20] See, for example, Ref. 9, pp. 501–541and Ref. 10, pp. 359–362.
[21] M. A. Doncheski and R. W. Robinett, "Anatomy of a quantum 'bounce'," Eur. J. Phys. **20**, 29–37 (1999).
[22] R. L. Hudson, "When is the Wigner quasiprobability density nonnegative?," Rep. Math. Phys. **6**, 249–252 (1974); F. Soto and P. Claverie, "When is the Wigner function of multidimensional systems nonnegative?," J. Math. Phys. **24**, 97–100 (1983).
[23] A. Kenfack and K. Zyczkowski, "Negativity of the Wigner function as an indicator of nonclassicality," J. Opt. B. **6**, 396–404 (2004).
[24] M. Belloni, M. A. Doncheski, and R. W. Robinett, "Wigner quasiprobability distribution for the infinite square well: Energy eigenstates and time-dependent wave packets," Am. J. Phys. **74**, 1183–1192 (2004).
[25] D. F. Styer, "Quantum revivals versus classical periodicity in the infinite square well," Am. J. Phys. **69**, 56–62 (2001).
[26] D. L. Aronstein and C. R. Stroud Jr., "Fractional wave-function revivals in the infinite square well," Phys. Rev. A **55**, 4526–4537 (1997).
[27] D. F. Styer, "The motion of wave packets through their expectation values and uncertainties," Am. J. Phys. **58**, 742–744 (1990).
[28] R. W. Robinett, "Visualizing the collapse and revival of wave packets in the infinite square well using expectation values," Am. J. Phys. **68**, 410–442 (2000).
[29] See, for example, Ref. 9, pp. 760–762.
[30] See, for example, Ref. 9, pp. 715–719.
[31] See, for example, Ref. 9, pp. 354–358, and Ref. 10, p. 163.
[32] V. G. Gueorguiev, A. R. P. Rau, and J. P. Draayer, "Confined one-dimensional harmonic oscillator as a two-mode system," Am. J. Phys. **74**, 394–403 (2006).
[33] See EPAPS Document No. E-AJPIAS-76-001804 for accompanying packages. This document can be reached through a direct link in the online article's HTML reference section or via the EPAPS homepage (http://www.aip.org/pubservs/epaps.html).
[34] ⟨http://www.compadre.org/quantum⟩.